IJE TRANSACTIONS A: Basics Vol. 29, No. 7, (July 2016) 985-994

International Journal of Engineering

Journal Homepage: www.ije.ir

Analysis of the Characteristics, Physical Concepts and Entropy Generation in a Turbulent Channel Flow Using Vortex Blob Method

B. Zafarmand*[a], M. Souhar[b], A. Hossein Nezhad[c]

[a] *Department of Mechanical Engineering, Institute of Energy & Hydro Technology (IEHT), Mashhad, Iran*
[b] *Department of Mechanical Engineering, University of Lorraine, Nancy, France*
[c] *Department of Mechanical Engineering, University of Sistan and Baluchestan, Zahedan, Iran*

PAPER INFO

Paper history:
Received 07 March 2016
Received in revised form 29 April 2016
Accepted 02 June 2016

Keywords:
Turbulent Flow
Channel Characteristics
Vortex Blob Method
Entropy Generation

ABSTRACT

In this paper, using vortex blob method (VBM), turbulent flow in a channel is studied and physical concepts of turbulence are obtained and discussed. At first, time-averaged velocities, $\bar{u}$ and $\bar{v}$, and then their fluctuations are calculated. To clarify turbulence structures, velocity fluctuations u' and v' are plotted. It is observed that turbulence structures occupy different positions and move with convection velocity. To verify the second law of thermodynamics, averaged vorticity and its fluctuations as well as averaged entropy and its fluctuations are calculated. Contours of these fluctuations (ω', s') show that their positions coincide with the positions of turbulence structures and both positions move with the same velocity. Correlation coefficient of velocity fluctuations between two points, and temporal correlation coefficient at a point, which have significant role in understanding physics of turbulence, are calculated and plotted. Having obtained these coefficients, time and spatial micro-scales and then turbulence energy dissipation rate (ε) are obtained. Also, spatial-temporal correlation coefficients is calculated and then for turbulence structures microscale of time (memory), micro-scale of spatial (size) and convection velocity of structures are found. These scales estimate their life and size. Having obtained dual correlation coefficients, spectral studies of the velocity fluctuations, u' and v', are performed, which include both frequency amplitude (related to temporal correlation coefficient) and wave number (related to special correlation coefficient). In fact, spectral study of fluctuations is Fourier transform (Cosine) of these fluctuations. Finally, dropping rate of this transform is compared with available data in turbulence literature. In this research, for the first time, the turbulence structures are visualized and presented by employing the vector of velocity fluctuations, vorticity and entropy generation fluctuations.

***doi**: 10.5829/idosi.ije.2016.29.07a.14*

1. INTRODUCTION

In recent years, there has been significant attention toward understanding the characteristics of turbulent flows. This is realized when unsteady equations of motion can be solved. The current methods include the solution of Reynolds momentum equations which needs auxiliary equations. Common important disadvantage of these methods is that the constants of models are not universal. However, compared to those methods, fewer problems exist in the methods such as large eddy simulation and random vortex method (RVM) in which vorticity distribution is modeled by a number of vortices with Lagrangian point of view. In Lagrangian formulation, motion of the particles are modeled as a system of ordinary differential equations, making their solution very easier [1-3]. In this method (RVM), motion of the vortices consists of two mechanisms including convection and diffusion. On the solid wall, vortices are produced resulting from satisfying boundary condition including zero tangential velocity, and then transferred into the main stream by the

*Corresponding Author's Email: br.zafarmand@gmail.com (B. Zafarmand)

Please cite this article as: B. Zafarmand, M. Souhar, A. Hossein Nezhad,Analysis of the Characteristics, Physical Concepts and Entropy Generation in a Turbulent Channel Flow Using Vortex Blob Method, International Journal of Engineering (IJE), TRANSACTIONSA: Basics Vol. 29, No. 7, (July 2016) 985-994

convection and diffusion. Transport by the diffusion occurs because of the random motion of the vortices.

Laitone [4] used random vortex method to predict numerically the growth of large-scale coherent vortex structure in the early stages of the development of turbulence in a two-dimensional co-flowing shear layer and determined RMS fluctuation in horizontal velocity. Cottet et al. [5] used the vortex-in-cell for the viscous diffusion scheme and compared with a spectral method for 128 grid points and concluded that the evolution of the energy spectrum, kinetic energy, dissipation, entropy and skewness were in excellent agreement. Totsuka and Obi [6] compared the spectral method with the vortex method using the core spreading method and a Laplacian model used in the moving particle semi-implicit (MPS)[7], which is similar to the redistribution method in vortex methods. Yokota et al. [8] applied the vortex method to the calculation of a decaying homogeneous isotropic turbulence and compared the results with a spectral method calculation. Blot et al. [9] simulated the flow pattern around downstream of a rectangular bluff body inside a Channel. Gagnon and Huang [10] studied the flow behavior inside channels with and without lateral injection, and finally Martins and Ghoniem [11] simulated the non-reacting flow in a bluff-body burner. In this later work, authors gave an overview of vortex interactions in axisymmetric mixing zones. Other applications of these schemes can be found in combustion (Sethion [12]), biomechanics (Mc Cracken and Peskin [13], and the simulation of the wind flow over buildings (Summers et al. [14]). Many of the above-mentioned works have validated RVM for moderate and high Reynolds number flows, validating them against experiments or other numerical method. These high Reynolds number validation studies confirm the capability of vortex methods to simulate accurately complex flows. Furthermore, the numerical convergence of this method for spatial and time discretization parameters is extensively explored separately.

The main advantage of random vortex method is that instant velocity distribution is calculated and then time averaged velocity and velocity fluctuations are found easily. Calculating velocity fluctuations help us to calculate characteristics of turbulent flow depending on these fluctuations. RVM has advantages and disadvantages. Some of its advantages include: (1) There is no simplification of the Equations. (2) Contrary to turbulence models, it does not need auxiliary Equations. (3) It is used for laminar and turbulent flows. (4) Employing Lagrangian method, it is used to calculate velocity in the high gradient regions. And some of its disadvantages include: (1) Because of employing Lagrangian method its computation time is high. (2) This method cannot be used for three dimensional flows, because this method is based on the two dimensional vorticity transport equation which is solved in two steps of convection and diffusion (in the 3D vorticity transport equation the source term exists that cannot be solved in two mentioned steps). Also, in this method, the equation should be solved in the transformed plane by Schwarz-Christoffel mapping that is a two dimensional mapping.

Various researches have been performed in the field of turbulent flows in channels. Rostami et al. [15] used a white light particle image velocimetry (WL-PIV) system in order to provide a cost-efficient and safe alternative to laser systems while keeping the accuracy limits required for hydraulic model tests. The accuracy and integrity of the experiments were validated by comparison to the results which were obtained with empirical models of the mean velocity and Reynolds stress distribution in the boundary layer. Javid and Mohammadi [16] focused on a hydraulic radius separation approach used to calculate the boundary shear stress in terms of bed and wall shear stress proposed in a trapezoidal channel. Bonakdari et al. [17] investigated the use of the Tsallis entropy to predict the shear stress distribution in rectangular channels. Given a definition of the Tsallis entropy, it is maximized using the probability density function, which then is used to attain a novel shear stress equation. It should be stated that in the mentioned papers, the mean quantities of characteristics are obtained but the turbulence characteristics are not investigated in detail such as temporal and spatial and spatial-temporal correlation of fluctuations, dissipation energy and etc. in which they play an important role in transport equation of turbulence quantities.

In this work, using random blob method velocity fluctuations are calculated. Then, by using these velocity fluctuations, turbulent flow characteristics are calculated including correlation coefficient between two points, temporal correlation coefficient and temporal–spatial correlation coefficients. Having obtained these coefficients, different scales of turbulence structures are estimated. In other words, scale and size of turbulence structures and time of their memory before losing their characteristics are calculated.

Energy dissipation always exists in a turbulent flow. Small and large eddies significantly increase energy dissipation. Entropy generation can be an indicator of energy dissipation. Having obtained instant velocity distribution and its gradients, instant entropy generation, time averaged entropy and entropy fluctuations are obtained. It is concluded that maximum entropy fluctuations occurs near the walls and decreases as distance from the wall increases.

This result can be shown with the calculation of vorticity in a constant grid similar to the grid used for entropy generation. Variation of averaged vorticity and its fluctuations is similar to those of entropy generation in that both of them are produced due to the rotation of fluid.

Wherever there is no rotation, there will be no entropy generation and no energy dissipation.

By employing the vector of velocity fluctuations, for the first time, the turbulence structures are visualized. After plotting the vector of velocity fluctuations, these structures are appeared in some parts of channel mostly near the walls. By demonstrating these structures in different time steps, it is observed that not only they are not stationary but also they are moving with a certain velocity which is named convection velocity (in turbulence literature). It should be noted that by plotting the velocity vector, these turbulence structures cannot be visible and only by plotting the velocity fluctuation this purpose can be achieved. Moreover, these structures are visualized by the use of vorticity fluctuations and entropy generation fluctuations.

2. GOVERNING EQUATIONS AND MODEL DESCRIPTION

The R.V.M is a numerical technique to solve unsteady Navier-Stokes equations converted to a rotational non-primitive formulation. These equations are the Poisson equation:

$$\nabla^2\psi = -\omega \tag{1}$$

and the vorticity transport equation is obtain by operating the curl of Navier-Stokes equations with considering the continuity equation $(\nabla.U = 0)$ as:

$$\frac{\partial\omega}{\partial t} + \mathbf{U}\cdot\nabla\omega = \frac{1}{\mathrm{Re}}\nabla^2\omega \tag{2}$$

where ω is dimensionless vorticity, $\mathbf{U}$ is the vector of velocity, $\mathrm{Re} = U_0H_0/\upsilon$ is the Reynolds number, U_0 is the magnitude of the inlet velocity of the channel, H_0 is the vertical distance between its two parallel walls, υ is kinematic viscosity and t is dimensionless time.

In this method, vorticity transport equation is solved at two stages including convection and diffusion [1] as follows.

$$\frac{\partial\omega}{\partial t} + \mathbf{U}\cdot\nabla\omega = 0 \tag{3}$$

$$\frac{\partial\omega}{\partial t} = \frac{1}{\mathrm{Re}}\nabla^2\omega \tag{4}$$

By solving Equations (3) and (4), vorticity transport equation solution is obtained. Equation (3) is solved using Lagrangian approach for vortices. This solution is performed using stream function ψ and Biot-Savart law as follows [1]:

$$U(X) = \iint k(X - X')\,\omega(X')dX' \tag{5}$$

$$k(X) = -\frac{1}{2\pi}\frac{(y,-x)}{r^2} \tag{6}$$

where, k is the kernel of Poisson equation for stream function, $dX' = dxdy$, and $r^2=x^2+y^2$. Equation (5) links velocity to vorticity distribution. Using Kelvin-Helmholtz theory, Equation (3) is written in an alternative form: If $\chi(x_0, t)$ denotes position of a particle passing the position x_0 at time t and $\omega(x_0)$ represents vorticity distribution at time t=0, then Equation (3) is expressed as:

$$\omega(\chi(x_0,t) = \omega(x_0) \tag{7}$$

where χ is the solution of the following equation:

$$\frac{d\chi}{dt} = U(\chi(x_0,t)) \quad with \quad \chi(x_0,t=0) = x_0 \tag{8}$$

In fact Equation (8) is a system of equations whose number is equal to the fluid particles number. To reduce the number of equations, vorticity field is replaced with finite number of vortex elements having a circulation Γ_i defined as

$$\Gamma_i = \iint \omega(X)dX = \omega(X_i)\,\delta A_i \tag{9}$$

where, δA_i is the area of each vortex. Using Core function [1] vorticity distribution is expressed as:

$$\omega(x,y) = \sum_{i=1}^{N}\Gamma_i\, f_\delta(x,y) \tag{10}$$

to omit singular point of each vortex, where f is a radial and symmetric function. Substituting Equation (10) into Equation (5) yields

$$U(x,y) = \sum_{i=1}^{N}\Gamma_i\, k_\delta(x-x_i, y-y_i) \tag{11}$$

where:

$$k_\delta(x,y) = -\frac{1}{2\pi}\frac{(y,-x)}{r^2}\kappa(\frac{r}{\delta}) \tag{12}$$

and

$$\kappa(r) = 2\pi\int_0^r rf(r)dr \tag{13}$$

where, δ is radius of each vortex, and κ denotes circulation function inside each vortex element. Chorin [1], and Ghoniem and Gagnon [2] defined f(r) as:

$$\begin{cases} f(r) = \dfrac{1}{2\pi r} & if \quad r \le \delta \\ f(r) = 0 & if \quad r > \delta \end{cases} \tag{14}$$

Now, using finite number of differential equations and Lagrangian approach, vortex motions are expressed as:

$$\frac{dX}{dt}=\sum_{i=1}^{N}\Gamma_i k_\delta(X_j-X_i) \qquad j=1,2,3,...,N \tag{15}$$

Substituting Equation (12) into Equation (15), induced velocity on j[th] vortex is calculated, which expressed in compact form as:

$$\overline{W}(z_j)=\sum_{\substack{i=1\\ i\neq j}}^{N}\frac{-i\Gamma_i|z_j-z_i|}{2\pi Max(|z_j-z_i|,\delta)}\frac{1}{z_j-z_i} \tag{16}$$

where, W=u+iv, z=x+iy, $i=\sqrt{-1}$, $\overline{w}$ is conjugate velocity and N is number of vortices. At the next step, transport of the vorticity of Equation (4) is performed with random convection of vortices based on a Gausian random variable. One-dimensional solution of Equation (4) is obtain by Green function as:

$$Gr(x,t)=\left(\sqrt{\frac{\mathrm{Re}}{4\pi t}}\,EXP\left(-\frac{\mathrm{Re}}{4t}x^2\right)\right) \tag{17}$$

which is similar to the density of Gauss probability function with random variable η, zero average and standard deviation σ:

$$P(\eta)=\left(\sqrt{\frac{1}{2\pi\sigma^2}}\,EXP\left(-\frac{1}{2\sigma^2}\eta^2\right)\right) \tag{18}$$

The two mentioned equations are the same if $\sigma=\sqrt{2t/\mathrm{Re}}$. Similarly, these procedures are applied to two-dimensional cases. Diffusion stage of vorticity transport consists of two perpendicular displacements which in fact are random variables with Gauss distribution, zero average, and standard deviation as $\sqrt{2\Delta t/\mathrm{Re}}$. In which Δt is time step. Therefore, if $z_j(t)$ denotes position of j[th] vortex at time t, its position at time $t+\Delta t$ is calculated as follows:

$$z_j(t+\Delta t)=z_j(t)+W\Delta t+\eta_j \tag{19}$$

where, $\eta_j=\eta_x+i\eta_y$ in which η_x and η_y are Gauss random variables and W is calculated as:

$$\overline{W}(z_j)=\left[\sum_{\substack{i=1\\ i\neq j}}^{N}W(\xi_j,\xi_i)-\sum_{i=1}^{N}W(\xi_j,\overline{\xi_i})+W_p(\xi_j)\right]F(\xi_j) \tag{20}$$

where the first term indicates the induction velocity of all vortices on j[th] vortex, the second term denotes induction velocity of the images of all vortices on j[th] vortex, and the third term is convective potential at Z_j, and $F(\xi)$ is Schwarz-Christoffel mapping function. As stated before, to impose zero normal velocity on the wall of polygonal geometries, conformal mapping of Schwarz-Christoffel and images of vortices are used. Conformal mapping of Schwarz-Christoffel for a two dimensional channel is as follows [3]:

$$F(\xi)=\frac{d\xi}{dz}=\frac{\pi}{H_0}\xi \tag{21}$$

$$\xi(z)=\mathrm{Exp}\left(\frac{\pi z}{H_0}\right) \tag{22}$$

$$z(\xi)=\frac{H_0}{\pi}\mathrm{Ln}(\xi) \tag{23}$$

where, $z=x+iy$ is a complex number that indicates a point in the channel and ξ is a point corresponding to the point z in the transformed plane. The inlet flow of the channel is simulated with a source located at the center point of the transformed plane and the outlet flow of it is simulated with a sink located at the infinity point of the transformed plane (Figure 1).

As already mentioned, the main goal of the present work is to solve the vorticity equation in the two stages of convection and diffusion. To satisfy zero tangential velocity on the walls, generation of similar vortices (having similar radius and circulation) is used. To satisfy zero normal velocity for the multi-lateral geometries, conformal mapping of Schwarz-Christoffel and vortex image are used.

Vortices produced on the walls as a result of satisfying zero tangential velocity leave the walls and enter into the flow by diffusion process, and then continue their motion by convection and diffusion means. The motion resulted from the diffusion of the vortices is composed of two perpendicular motions. These two motions are random variables with zero mean Gauss distribution and standard deviation of $\sqrt{2\Delta t/\mathrm{Re}}$.

3. RESULTS AND ANALYSIS

3. 1. Calculation of Average Velocity Field

When vortices occupies almost entirely the computational domain and their number approaches a constant limit, fluid velocity can be calculated in a constant grid. This velocity is composed of velocity of potential flow and velocity induced by vortices and their images.

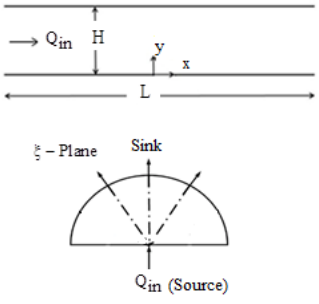

Figure 1. Demonstration of physical plane (z) and transformed plane (ξ)

In order to show the power of random vortex method, velocity field of a laminar flow with Re=250 is calculated. Figure 2 shows the comparison between the velocity field of this case resulted from the present work and parabolic profile of the fully developed flow. The results show good agreement. In this flow standard deviations of the velocity fluctuations are very small, actually are zero.

For turbulent flow with $Re = 50000$, after calculating instant velocities on a constant grid, time averaged velocity in the interval of 400 time steps by using the following formula is calculated.

$$\bar{W} = \frac{\sum_{j=1}^{M} w_j}{M} \quad (24)$$

where, $w = u + iv$ is complex velocity of the fluid and M is the number of time steps. Figure 3 illustrates axial velocity profile and compares it with velocity distribution of Prandtl's power law (n=7) in different sections and a good agreement between them is observed.

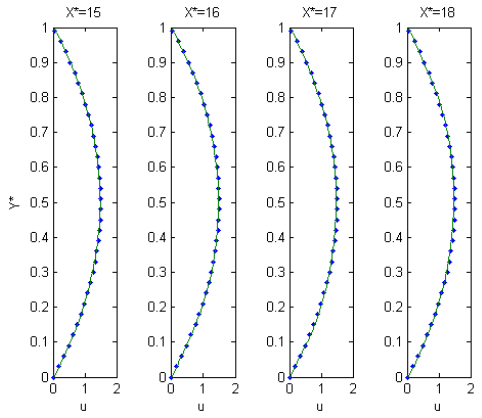

Figure 2. Comparison between the velocity profile of the present model and analytical solution (indicated with the symbol *) at Re=250 in four sections

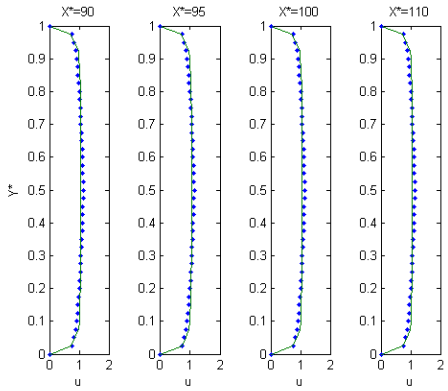

Figure 3. Comparison between the velocity profile of the present model with velocity distribution of Prandtl's power law (n=7) (indicated with the symbol *) at Re=50000 in four sections

3. 2. Calculation of Velocity Fluctuations After calculating instant velocity and time-averaged velocity, velocity fluctuations is calculated using the relation $w'(t) = w(t) - \bar{w}$ in which $w' = u' + iv'$. Having calculated velocity fluctuations, standard deviations of them and Reynolds stresses can be calculated. Moreover, by using them, small structures of turbulence can be illustrated.

Figure 4 shows variation of $\sqrt{\overline{u'^2}}$, $\sqrt{\overline{v'^2}}$ and $\overline{u'v'}$, which were made non dimensional by mass average velocity in the channel at $x^* = 90$. Although small turbulence structures can not be illustrated by plotting instant velocities, they can be shown very easily by plotting velocity fluctuations. Therefore, velocities must be calculated in a fine grid. A grid is assumed from $x^* = 90$ with $\Delta x^* = \Delta y^* = 0.01$. After calculating velocity fluctuations in the constant grid, their velocity vectors are plotted. It is seen that small vortices are being formed and moves with a specific velocity and then disappear after moving some distance. Also, the scale of structures is different.

Figure 5 depicts the movements of the vortices plotted at two different times. After calculating velocities of the vortices named as convection velocities, it is observed that their values are approximately as much as 0.8 times the maximum velocity of the fluid in the channel and agree favorably with experimental data of Souhar [18] and Sabot [19].

3. 3. Calculation of Correlation Coefficients Correlation coefficients between the two points play an important role in the theory of turbulence. Using these coefficients, scales of turbulence showing schematic organization of turbulent flow are found. In addition, these coefficients are effective in the averaged Reynolds equations.

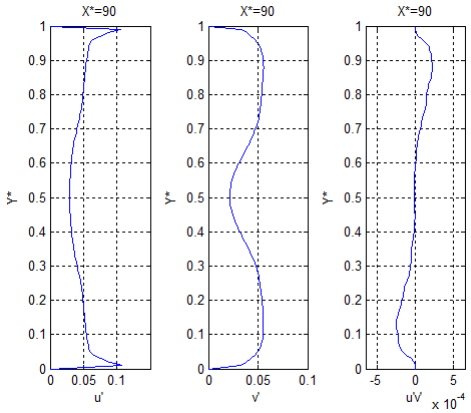

Figure 4. Variations of $\sqrt{\overline{u'^2}}$, $\sqrt{\overline{v'^2}}$ and $\overline{u'v'}$, made non-dimensional by mass average velocity in the channel versus Y^* at x^*=90

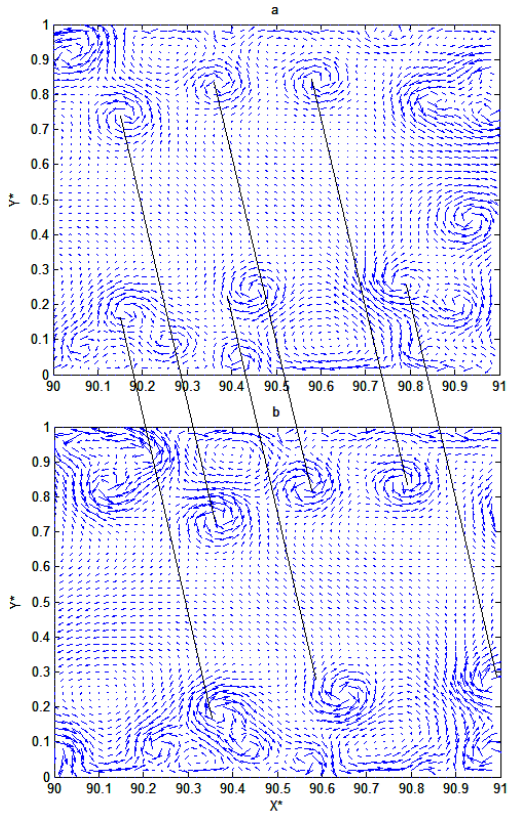

Figure 5. Vector plots of velocity fluctuations and demonstration of turbulence structures at two different times (a) $310\Delta t$, (b) $312\Delta t$

Dual spatial correlation coefficient indicates the existence of large turbulence structures, and temporal one shows the existence of the memory for vortex and indicates its life time.

Spatial correlation of velocity fluctuation components between two points A and B in the physical domain with $\vec{x}_B - \vec{x}_A = \vec{r}$, in the time t is defined as follows [20]:

$$R_{ij}(\vec{x}_A, \vec{r}, t) = \frac{\overline{u'_{iA}(t)u'_{jB}(t)}}{\sqrt{\overline{u'^2_{iA}}}\sqrt{\overline{u'^2_{jB}}}} \quad (25)$$

and temporal correlation of velocity fluctuation at point A in the time interval t and $t+\tau$ in which τ is delay time is defined as follows:

$$R_{ij}(\vec{x}_A, t, \tau) = \frac{\overline{u'_{iA}(t)u'_{jA}(t+\tau)}}{\sqrt{\overline{u'^2_{iA}(t)}}\sqrt{\overline{u'^2_{jA}(t+\tau)}}} \quad (26)$$

For a small delay time, using Taylor expansion gives:

$$R_{ii}(\tau) = 1 - \frac{\tau^2}{2\lambda_{it}^2} \quad , \quad \frac{1}{\lambda_{it}^2} = -\frac{1}{2}\left(\frac{\partial^2 R_{ii}(\tau)}{\partial \tau^2}\right)_{\tau=0} \quad (27)$$

Where λ_{it} is time micro-scale or Taylor scale in the direction i which is obtained by using osculatrice parabola.

The second time scale is $T_i = \int_0^\infty R_{ii}(\tau)d\tau$ referred to as macro-scale or integral scale and indicates a time which after that, velocities are not correlated with each other. λ_{it} is not the lower limit of time for the decaying of small-scale structures of turbulence, which depend to Kolmogorov time micro-scale. If turbulent flow is assumed at least locally homogeneous and isotropic, spatial correlation coefficient does not depend on the chosen point:

$$R_{ii}(r) = \frac{\overline{u'_i(0,t)u'_i(r,t)}}{\sqrt{\overline{u'^2_i(0,t)}}\sqrt{\overline{u'^2_i(r,t)}}} \quad (28)$$

Similarly, for small r using Taylor expansion gives:

$$R_{ii}(r) = 1 - \frac{r^2}{2\lambda_{ir}^2} \quad , \quad \frac{1}{\lambda_{ir}^2} = -\frac{1}{2}\left(\frac{\partial^2 R_{ii}(r)}{\partial r^2}\right)_{r=0} \quad (29)$$

where λ_{ir} is spatial micro-scale. The second spatial scale is $L_{ii} = \int_0^\infty R_{ii}(r)dr$ known as spatial macro-scale. For a homogeneous, isotropic turbulent flow the relation between $R_{11}(r)$ and $R_{22}(r)$ is as [20]:

$$R_{22}(r) = R_{11}(r) + \frac{1}{2}r\frac{\partial R_{11}(r)}{\partial r} \quad , \quad \lambda_f = \lambda_g\sqrt{2} \quad (30)$$

where, $R_{11}(r)$ and $R_{22}(r)$ are respectively correlation coefficients of u' and v' in the longitudinal direction, λ_f and λ_g are respectively micro-scales of u' and v', obtained by the intersection of osculatrice parabola with horizontal axis. The physical importance of Taylor micro-scale is that by using it, dissipation rate (ε) can be obtained as:

$$\varepsilon = 30\upsilon\frac{\overline{u'^2}}{\lambda_f^2} = 15\upsilon\frac{\overline{u'^2}}{\lambda_g^2} \quad (31)$$

Figure 6 demonstrates the variations of temporal correlation coefficients of velocity fluctuations u' i.e. $R_{11}(\tau)$ and v' i.e. $R_{22}(\tau)$ versus time. Figure 7 shows variations of spatial correlation coefficients of velocity fluctuations u' i.e. $R_{11}(r)$ and v' i.e. $R_{22}(r)$ in the center of the channel and $x^* = 90$ versus distance between two points r. The intersection of osculatrice parabola with horizontal axis shows spatial micro-scale. Figure 8 depicts variations of correlation coefficient of velocity fluctuations v' i.e. $R_{22}(r)$ in the center of the channel and its comparison with $R_{22}(r)$ obtained from isotropic relation. It is observed that at small distances between two points, turbulent flow is locally isotropic, and as the distance between two points increases,

deviation from isotropic turbulence becomes larger. As already mentioned, by knowing the correlation coefficients, the spatial and temporal micro-scales $(\lambda_{ir}, \lambda_{it})$ can be obtained by employing the osculating parabola. The dissipation rate (ε) which has an important role in turbulent flows, can be achieved by using these micro-scales (Equation (31)). Also, Figure 8 shows in little distance $(r < 0.2)$ that the behavior of turbulence is isotropic and homogenous which allows to use Equation (31) for calculating the dissipation rate.

3. 4. Calculation of Spatial-temporal Correlation Reduction of spatial-temporal correlation coefficient $R_{11}(r,0,0,\tau_m)$ related to longitudinal velocity fluctuation u' can be calculated.

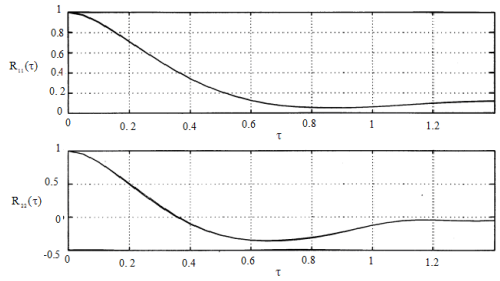

Figure 6. Variations of temporal correlation coefficients of velocity fluctuations u' i.e. $R_{11}(\tau)$ and v' i.e. $R_{22}(\tau)$ in the center of the channel and $X^* = 90$

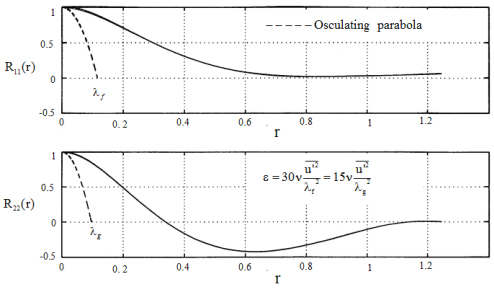

Figure 7. Variations of spatial correlation coefficients of velocity fluctuations u' i.e. $R_{11}(r)$ and v' i.e. $R_{22}(r)$ in the center of the channel and $X^* = 90$, and demonstration of turbulence micro-scales

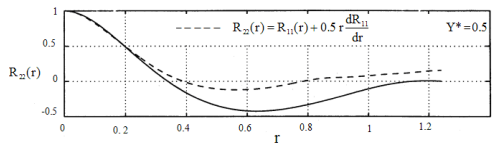

Figure 8. Variations of correlation coefficient of velocity fluctuations v' i.e. $R_{22}(r)$ and its comparison with $R_{22}(r)$ obtained from isotropic relation in the center of the channel and $X^* = 90$

Figure 9 shows the spatial-temporal correlation coefficient in the center of the channel. In this figure, $r = 0$ coincides with $x^* = 90$, and $r = 1, 2, ..., 10$ denotes different distances from that point. Each of the curves of $R_{11}(r,0,0,\tau_m)$ depends to r and has a maximum which occurs at τ_m. In fact, the curves passing through maximum points show variation of $R_{11}(\tau_m)$ versus τ_m. It is observed that $R_{11}(\tau_m)$ approaches uniformly to zero. Obtaining this curve, scale of time integral is calculated from the following relation [20]:

$$\theta_{11} = \int_0^{\infty} R_{11}(\tau_m) d\tau_m \tag{32}$$

where, θ_{11} is temporal correlation (memory time) of the longitudinal velocity fluctuations. Using this, length macro-scale is calculated as follows:

$$L_{11} = \sqrt{\overline{u'^2}}\,\theta_{11} \tag{33}$$

At the distance r, convection velocity is defined as $U_c = r/\tau_m$. At large r, convection velocity approaches to a limit value $U_{c,l}$ which is an index for the velocity of turbulence structures. The curves of Figure 9 shows this velocity is 0.8 times as much as the maximum velocity of the flow in the channel.

3. 5. Calculation of Vorticity The most important quantity that distinguish real and rotational flow from ideal and potential flow is vorticity vector . Similarly, instant vorticity can be calculated using instant velocity field and its gradients, and then time averaged vorticity $\bar{\omega}$ and its fluctuation ω' can be found. Therefore, in a constant grid, using above equation and instant velocity field calculated before, vorticity field was calculated.

3. 6. Calculation of Entropy Generation The second law of thermodynamics is a basic law governing all processes and flows. Here, the turbulent structures form this points of view is investigated. In an adiabatic process, entropy generation per unit volume and per unit time in non- dimensional form is calculated from the following relation.

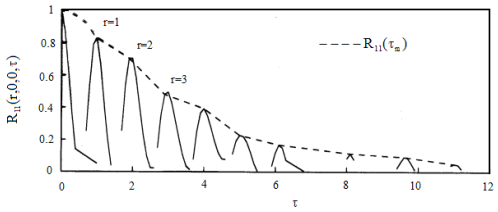

Figure 9. Variations of spatial-temporal correlation coefficient in the center of the channel and X^*=90

$$S=\frac{1}{Re}\left\{2\left[\left(\frac{\partial u}{\partial X^*}\right)^2+\left(\frac{\partial v}{\partial Y^*}\right)^2\right]+\left(\frac{\partial u}{\partial Y^*}+\frac{\partial v}{\partial X^*}\right)^2\right\} \quad (34)$$

where, S defined as:

$$S=\frac{S'''_{gen}}{\rho U_0^3/T_0H_0} \quad (35)$$

in which, T_0 is fluid temperature and S'''_{gen} is entropy generation per unit volume and per unit time. Again, using instant velocity distribution and its gradients, instant entropy generation, time averaged entropy $\overline{S}$ and its fluctuations $S'(t)$ can be evaluated. The entropy generation was calculated in a constant grid used for the calculation of vorticity.

Figure 10 illustrates the turbulent structures resulted respectively from plotting velocity fluctuations, contours of vorticity fluctuation ω', and contours of entropy generation fluctuation $S'(t)$ in a specific time. It is concluded that:

(1) Position and rotation center of each structure is the same in the three curves. In other words, information of each turbulence structure can be found from distribution of velocity fluctuations, contours of vorticity fluctuation ω', and contours of entropy fluctuation $S'(t)$.

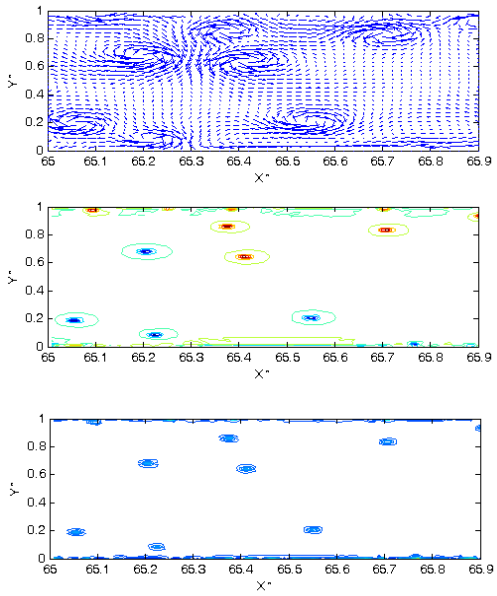

Figure 10. Demonstration of turbulent structures obtained respectively from plotting velocity fluctuations, contours of vorticity fluctuation $\omega'(t)$, and contours of entropy generation fluctuation $S'(t)$

(2) Because of high velocity gradients near the walls, large scale turbulence structures are located in this regions and rarely seen in the central region.
(3) It seems that turbulence structures are circular. By using the contours of vorticity fluctuation ω'
(4) If in a region vorticity fluctuations is high, entropy generation and as a result dissipation rate are high in that region.

3. 7. Spectral Analysis of Velocity Fluctuations

Studying physics of the turbulent flow is performed in frequency domain or wave numbers [20]:

$$E(f^*)=\frac{1}{2\pi}\int_0^{\infty}\overline{u'^2}R(\tau)Cos(f^*\tau)d\tau \quad (36)$$

where f^* is non-dimensional frequency, and $E(f^*)$ is density of spectral energy. Therefore, obtaining temporal correlation coefficient, makes possible the spectral study of u'^2. Furthermore, for an isotropic turbulence Fourier analysis gives:

$$E_{11}(k^*)=\frac{1}{\pi}\int_0^{\infty}\overline{u'^2}R_{11}(r)Cos(k^*r)dr \quad (37)$$

$$E_{22}(k^*)=\frac{1}{\pi}\int_0^{\infty}\overline{v'^2}R_{22}(r)Cos(k^*r)dr \quad (38)$$

where, $E_{ii}(k^*)$ is Cosine Fourier transform and k^* is non-dimensional wave number. It should be stated that by obtaining correlation coefficients of velocities, their spectrums can be evaluated. While energy decreases, there is a region in which dissipation rate ε is constant, known as equilibrium region. In this region energy spectrum does not depends to molecular viscosity and is governed by the following general law [20]:

$$E\propto\varepsilon^{\frac{2}{3}}(k^*)^{-\frac{5}{3}} \quad (39)$$

After this region energy varies as:

$$E\propto(k^*)^{-4} \quad (40)$$

Figure 11 shows spectral density of energy for u'^2 and v'^2 in the frequency domain, and Figure 12 shows spectral energies of u'^2 and v'^2 in the longitudinal direction at different distances of Y^*. Having obtained correlation coefficients, these quantities are calculated and plotted. In all of these curves, lines with slope of -5/3 and -4 are drawn and it is seen that by approaching to the channel center, the slope of energy drop approaches to the isotropic turbulence and shows an acceptable agreement.

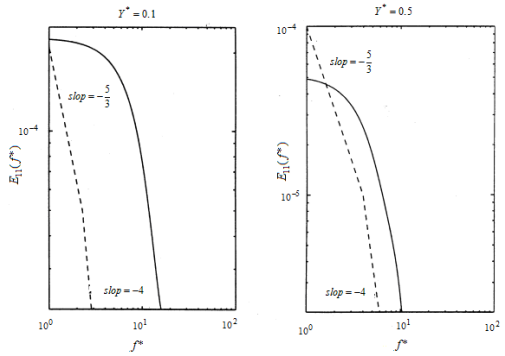

Figure 11. Spectral density of energy for u'^2 and v'^2 in longitudinal direction near the wall and in the center of the channel

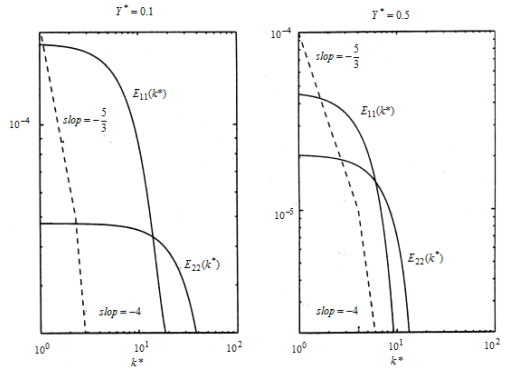

Figure 12. Spectral energies of u'^2 and v'^2 in longitudinal direction near the wall and in the center

4. CONCLUSION

Most of the previous studies have been carried out only to calculate the time averaged velocities. However, in this work, using vortex blob method, which despite of its simplicity is very exact, a comprehensive study of a turbulent flow inside a two dimensional channel was performed to give a better understanding of the characteristics and physical concepts of turbulent flow. For this purpose, having calculated velocity fluctuations, spatial correlation coefficient between two points, temporal correlation coefficient at a point, and then time and spatial micro-scales were calculated. Importance of the micro-scales is in that when turbulent flow is locally turbulent, dissipation rate can be obtained after calculating them. Time micro-scale indicates a time after which velocities are not connected with each other. Spatial macro-scale is an indicative of the size of the turbulence structures. Turbulence structures were shown by plotting contours of vorticity fluctuations. These structures were also shown by plotting velocity fluctuations vectors and plotting contours of entropy fluctuations. In fact second law of thermodynamics verifies energy dissipation of turbulent flow and states that this dissipation is due to the generation and decaying of turbulence structures in the channel flow, which often occurs near the walls. By calculation and plotting components of Reynolds stress tensor in the fully developed region it was shown that turbulent intensity is larger near the walls than that of other places of the channel. After calculating velocities of the vortices named as convection velocities, it is observed that their values are approximately as much as 0.8 times the maximum velocity of the fluid in the channel and agree favorably with experimental data. Using Fourier Transform, spectral frequencies or wave number of velocity fluctuations was calculated and plotted. It was observed that energy variation is proportional to the power of -5/3 of the wave number in a narrow band, while it is proportional to power of-4 of the wave number in a broad band. These results demonstrate a good agreement with the turbulence literature.

5. REFERENCES

1. Chorin, A.J., "Numerical study of slightly viscous flow", ***Journal of Fluid Mechanics***, Vol. 57, No. 04, (1973), 785-796.
2. Ghoniem, A.F. and Cagnon, Y., "Vortex simulation of laminar recirculating flow", ***Journal of Computational Physics***, Vol. 68, No. 2, (1987), 346-377.
3. Zafarmand, B., "Simulation numerique des ecoulements turbulents et a bulles dans un canal simple et dans un te par la methode des vortex aléatoires", Vandoeuvre-les-Nancy, INPL, (1996),
4. Laitone, J., "Numerical experiments on turbulent flow using the random vortex method", ***International Journal for Numerical Methods in Engineering***, Vol. 24, No. 7, (1987), 1297-1303.
5. Cottet, G.-H., Michaux, B., Ossia, S. and VanderLinden, G., "A comparison of spectral and vortex methods in three-dimensional incompressible flows", ***Journal of Computational Physics***, Vol. 175, No. 2, (2002), 702-712.
6. Totsuka, Y. and Obi, S., The vortex method applied to simulation of homogeneous isotropic turbulence, in Computational methods. 2006, Springer.1503-1508.
7. Koshizuka, S., "A particle method for incompressible viscous flow with fluid fragmentation", ***Computer Fluid Dynamics Journal***, Vol. 4, (1995), 29-46.
8. Yokota, R., Sheel, T.K. and Obi, S., "Calculation of isotropic turbulence using a pure lagrangian vortex method", ***Journal of Computational Physics***, Vol. 226, No. 2, (2007), 1589-1606.
9. Blot, F., Giovannini, A., Hebrard, P. and Strzelecki, A., "Flow analysis in a vortex flowmeter-an experimental and numerical approach", in 7th Symposium on Turbulent Shear Flows, Volume 1. Vol. 1, (1989), 21-23.
10. Gagnon, Y. and Huang, W., "Fast vortex method for the simulation of flows inside channels with and without injection", ***Journal of Thermal Science***, Vol. 2, No. 1, (1993), 1-11.
11. Martins, L.-F. and Ghoniem, A.F., "Simulation of the nonreacting flow in a bluff-body burner; effect of the diameter ratio", ***Journal of Fluids Engineering***, Vol. 115, No. 3, (1993), 474-484.

12. Sethian, J.A. and Ghoniem, A.F., "Validation study of vortex methods", ***Journal of Computational Physics***, Vol. 74, No. 2, (1988), 283-317.
13. McCracken, M. and Peskin, C., "A vortex method for blood flow through heart valves", ***Journal of Computational Physics***, Vol. 35, No. 2, (1980), 183-205.
14. Summers, D., Hanson, T. and Wilson, C., "A random vortex simulation of wind-flow over a building", ***International Journal for Numerical Methods in Fluids***, Vol. 5, No. 10, (1985), 849-871.
15. Rostami, M., Ardeshir, A., Ahmadi, G. and Thomas, P.J., "Development of a low cost and safe piv for mean flow velocity and reynolds stress measurements", ***International Journal Of Engineering Transactions A Basics***, Vol. 20, No. 2, (2007), 105-116.
16. Javid, S. and Mohammadi, M., "Boundary shear stress in a trapezoidal channel", ***International Journal of Engineering-Transactions A: Basics***, Vol. 25, No. 4, (2012), 323-331.
17. Bonakdari, H., Tooshmalani, M. and Sheikh, Z., "Predicting shear stress distribution in rectangular channels using entropy concept", ***International Journal of Engineering-Transactions C: Aspects***, Vol. 28, No. 3, (2014), 360-367.
18. Souhar, M., "Contribution a l'etude dynamique des ecoulements diphasiques gaz-liquide en conduite verticale: Cas des regimes a bulles et a poches", (1982).
19. Sabot, J., "Etude de la coherence spatiale et temporelle de la turbulence etablie en conduite circulaire", (1976),
20. Hinze, J., "Turbulence mcgraw-hill", ***New York***, Vol. 218, (1975).

Analysis of the Characteristics, Physical Concepts and Entropy Generation in a Turbulent Channel Flow Using Vortex Blob Method

B. Zafarmand[a], M. Souhar[b], A. Hossein Nezhad[c]

[a] *Department of Mechanical Engineering, Institute of Energy & Hydro Technology (IEHT), Mashhad, Iran*
[b] *Department of Mechanical Engineering, University of Lorraine, Nancy, France*
[c] *Department of Mechanical Engineering, University of Sistan and Baluchestan, Zahedan, Iran*

P A P E R I N F O

Paper history:
Received 07 March 2016
Received in revised form 29 April 2016
Accepted 02 June 2016

Keywords:
Turbulent Flow
Channel Characteristics
Vortex Blob Method
Entropy Generation

چکیده

در این مقاله با استفاده از گردابه‌های تصادفی به بررسی جریان درهم در داخل یک کانال و استخراج مفاهیم فیزیکی جریان آشفته پرداخته شده است. در ابتدا سرعت‌های متوسط زمانی $\bar{u}$ ، $\bar{v}$ و سپس نوسان‌های آنها محاسبه می‌گردند. به منظور واضح نمودن ساختارهای جریان آشفته، بردارهای نوسانات سرعت طولی و عرضی u' و v' رسم شدند و دیده شد که در زمان‌های مختلف، ساختارها در موقعیت‌های مختلف قرار می گیرند. به عبارت دیگر با سرعت مشخصی (Convection Velocity) درحرکت هستند. همچنین کمیت ورتیسیته متوسط و نوسان‌های آن محاسبه می‌شوند و برای نشان دادن تأیید قانون دوم ترمودینامیک در جریان آشفته، تولید آنتروپی متوسط و نوسان‌های آن نیز در مقاطع مختلف محاسبه می‌گردند. رسم کانتورهای نوسانات ورتیسیته و آنتروپی (ω' , s') نشان می‌دهند که موقعیت آنها دقیقاً منطبق برموقعیت ساختارهای جریان آشفته بوده و با همان سرعت جابجایی در حرکت هستند. ضریب همبستگی نوسانات سرعت در دو نقطه و ضریب همبستگی زمانی در یک نقطه (Correlation) که در تئوری فیزیکی جریان آشفته نقش اساسی و مهمی دارند نیز محاسبه و رسم می‌شوند. با داشتن این ضرایب، میکرواشل‌های زمانی و مکانیساختمان‌های (Structures) جریان آشفته محاسبه می‌شوند که با استفاده از آنها ε تلفات انرژی (Dissipation) نیز استخراج می-گردد. همچنین ضرایب همبستگی مکانی- زمانی (Spatial-Temporal) نیز محاسبه و از آنجا ماکرواشل زمانی (حافظه)، ماکرواشل مکانی (اندازه) و سرعت جابجایی ساختارهای جریان آشفته مشخص می‌شوند. این مقیاس‌ها به ترتیب زمان حیات گردابه ها و اندازه وبزرگی آنها را تخمین می زنند. هم‌چنین با داشتن ضرایب همبستگی دوگانه، مطالعه طیفی (Spectral) نوسانات سرعت u' و v' نیز انجام می‌گیرد که شامل دو دامنه فرکانسی (مربوط به ضریب همبستگی زمانی) و عدد موج (مربوط به ضریب همبستگی مکانی) می باشد. در واقع بررسی طیفی نوسانات عبارت است از تبدیل فوریه (کسینوس) این نوسانات. آهنگ سقوط این تبدیل با مقادیر موجود در مقالات مربوط به جریانات آشفته مقایسه شده‌است.

***doi**: 10.5829/idosi.ije.2016.29.07a.14*